Catalysis of Protein Disulfide Bond Isomerization in a Homogeneous Substrate†

Elizabeth A. Kersteen,‡,§ Seth R. Barrows,‡ and Ronald T. Raines*,‡,||

Departments of Biochemistry and Chemistry, University of Wisconsin−Madison, Madison, Wisconsin 53706

Received April 29, 2005; Revised Manuscript Received July 1, 2005

ABSTRACT: Protein disulfide isomerase (PDI) catalyzes the rearrangement of nonnative disulfide bonds in the endoplasmic reticulum of eukaryotic cells, a process that often limits the rate at which polypeptide chains fold into a native protein conformation. The mechanism of the reaction catalyzed by PDI is unclear. In assays involving protein substrates, the reaction appears to involve the complete reduction of some or all of its nonnative disulfide bonds followed by oxidation of the resulting dithiols. The substrates in these assays are, however, heterogeneous, which complicates mechanistic analyses. Here, we report the first analysis of disulfide bond isomerization in a homogeneous substrate. Our substrate is based on tachyplesin I, a 17-mer peptide that folds into a β hairpin stabilized by two disulfide bonds. We describe the chemical synthesis of a variant of tachyplesin I in which its two disulfide bonds are in a nonnative state and side chains near its N and C terminus contain a fluorescence donor (tryptophan) and acceptor (N_ϵ-dansyllysine). Fluorescence resonance energy transfer from 280 to 465 nm increases by 28-fold upon isomerization of the disulfide bonds into their native state (which has a lower $E^{\circ\prime} = -0.313$ V than does PDI). We use this continuous assay to analyze catalysis by wild-type human PDI and a variant in which the C-terminal cysteine residue within each Cys-Gly-His-Cys active site is replaced with alanine. We find that wild-type PDI catalyzes the isomerization of the substrate with $k_{cat}/K_M = 1.7 \times 10^5$ M^{-1} s^{-1}, which is the largest value yet reported for catalysis of disulfide bond isomerization. The variant, which is a poor catalyst of disulfide bond reduction and dithiol oxidation, retains virtually all of the activity of wild-type PDI in catalysis of disulfide bond isomerization. Thus, the C-terminal cysteine residues play an insignificant role in the isomerization of the disulfide bonds in nonnative tachyplesin I. We conclude that catalysis of disulfide bond isomerization by PDI does not necessarily involve a cycle of substrate reduction/oxidation.

Disulfide bonds between half-cystine residues are the only common cross-links in native proteins (*1*−*3*). During the oxidative folding of proteins, disulfide bonds are likely to form between those cysteine residues that are most proximal in the amino acid sequence (*4*).[1] For a protein to fold properly, however, these nascent disulfide bonds must rearrange to the half-cystine pairings of the native conformation.

In eukaryotic cells, the formation of native disulfide bonds is catalyzed by protein disulfide isomerase [PDI[2] (*8*−*13*)]. This 55-kDa enzyme contains four distinct structural domains (a, a′, b, and b′) that are homologous to thioredoxin and an acidic C-terminal domain (c) (*14*−*16*). The a and a′ domains each contain a Cys-Gly-His-Cys (CGHC) active-site motif that catalyzes thiol−disulfide interchange reactions leading to the oxidation of dithiols and the reduction and isomerization of disulfide bonds (*8*). The role of the b domain is unclear but likely includes maintaining the structural integrity of the enzyme (*17*). The b′ domain does not contain catalytic residues but is required for substrate recognition and binding (*17*−*19*). The c domain contains a (K/H)DEL sequence that serves to maintain PDI in the endoplasmic reticulum (*20*).

PDI is essential for the viability of *Saccharomyces cerevisiae* (*21*−*24*). Still, there has been much debate over which of its cellular roles is necessary for survival (*25*−

† E.A.K. and S.R.B. were supported by Biotechnology Training Grant GM08349 (NIH). E.A.K. was also supported by WARF and Steenbock predoctoral fellowships. This work was supported, in part, by Grants BES 04563 (NSF) and GM44783 (NIH). The University of Wisconsin−Madison Biophysics Instrumentation Facility was supported by Grants BIR-9512577 (NSF) and RR13790 (NIH).

* To whom correspondence should be addressed: Department of Biochemistry, University of Wisconsin−Madison, 433 Babcock Drive, Madison, WI 53706-1544. Telephone: (608) 262-8588. Fax: (608) 262-3453. E-mail: raines@biochem.wisc.edu.

‡ Department of Biochemistry.

§ Current address: EraGen Biosciences, 918 Deming Way, Madison, WI 53717-1944.

|| Department of Chemistry.

[1] The reduction potential of a disulfide bond within an unstructured polypeptide chain can be estimated from polymer theory and empirical constants to be $E^{\circ\prime}$ (V) = −0.25 + (0.44)log(n), where n is the number of residues between the two-half cystines (*5*, *6*). This relationship is known not to apply strictly for $n \leq 5$ (*7*), presumably because of overriding steric constraints.

[2] Abbreviations: Acm, acetamidomethyl; AgOTf, silver trifluoromethanesulfonate; BPTI, bovine pancreatic trypsin inhibitor; DIEA, *N*,*N*-diisopropylethylamine; DMF, dimethylformamide; DMSO, dimethyl sulfoxide; dns, dansyl or 5-(dimethylamino)-1-naphthyl; dns-sTI, dansylated scrambled tachyplesin I; dns-nTI, dansylated native tachyplesin I; $E^{\circ\prime}$, standard reduction potential at pH 7.0; EDT, 2-ethanedithiol; F, fluorescence emission; F_0, substrate fluorescence; F_{max}, product fluorescence; Fmoc, fluorenylmethoxycarbonyl; FPLC, fast protein liquid chromatography; FRET, flourescence resonance energy transfer; GSH, reduced glutathione; GSSG, oxidized glutathione; HPLC, high-performance liquid chromatography; IPTG, isopropyl-1-thio-β-D-galactoside; LB, Luria−Bertani; MALDI−TOF, matrix-assisted laser desorption/ionization time-of-flight; PDI, protein disulfide isomerase; poly(C), poly(cytidylic acid); RNase A, bovine pancreatic ribonuclease; sRNase A, scrambled RNase A; TB, terrific broth; TFA, trifluoroacetic acid; TI, tachyplesin I; Trt, trityl.

10.1021/bi0507985 CCC: $30.25
Published on Web 08/16/2005

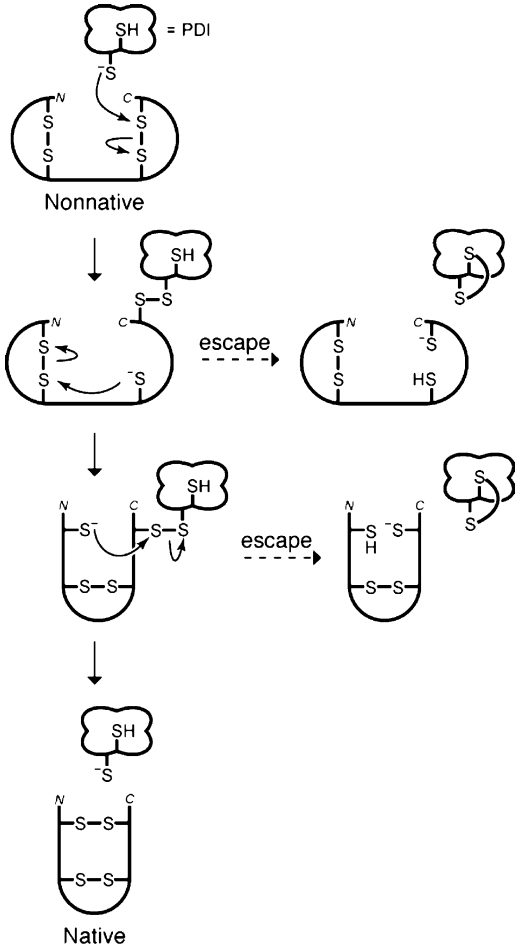

FIGURE 1: Putative mechanism of disulfide bond isomerization by PDI. The reaction begins with nucleophilic attack of an enzymic thiolate on a nonnative disulfide bond. Thiol−disulfide interchange reactions within the substrate ultimately produce native disulfide bonds and regenerate PDI. If a mixed disulfide intermediate becomes trapped, the other enzymic thiolate initiates an "escape" mechanism. Subsequent oxidation of the substrate and reduction of the enzyme would then be necessary to produce native disulfide bonds and regenerate PDI.

27). A variant of rat PDI in which both active sites contain a CGHS sequence, instead of CGHC, restores viability to *pdi1*Δ *S. cerevisiae* (*28*). *In vitro*, this PDI variant is proficient in catalysis of disulfide bond isomerization but has low dithiol oxidation and disulfide reduction activity (*28*, *29*). Further, PDI homologues, including Eug1p and variants of thioredoxin, which are inefficient catalysts of disulfide bond formation and reduction but can catalyze disulfide bond rearrangement, are able to rescue *pdi1*Δ *S. cerevisiae* (*30*, *31*). Recently, however, Gilbert and co-workers examined the effects of variable expression levels of yeast PDI variants on the growth and viability of *pdi1*Δ *S. cerevisiae* (*32*−*34*). Their results suggest that the oxidase activity of PDI limits growth and that isomerization might not limit the folding rate of proteins essential for yeast viability. Still, for many secretory proteins, the isomerization of nonnative disulfide bonds is known to be the slowest step in protein folding (*35*).

The mechanism by which PDI catalyzes disulfide bond isomerization likely involves the nucleophilic attack of the reactive N-terminal thiolate of the CGHC motif on a nonnative substrate disulfide to form a mixed disulfide intermediate (Figure 1). The resulting substrate thiolate is then free to attack a nonnative substrate disulfide. Further substrate rearrangements continue until the native disulfide bonds are reached and PDI is released without any net reduction or oxidation. Under some conditions, substrate thiolates could be incapable of completing the required disulfide rearrangements, in effect trapping an enzyme−substrate mixed disulfide. The C-terminal cysteine residue of the CGHC motif plays a critical role in rescuing these unproductive intermediates by forming an active-site disulfide bond and releasing a reduced substrate (*29*, *36*, *37*). Cycles of reduction and reoxidation would ultimately produce native protein. Although PDI was discovered over 40 years ago (*38*), the catalytic mechanism of disulfide bond isomerization is not well-understood. In particular, a key question remains about the steps that follow the formation of the initial mixed disulfide (Figure 1): Is the ability to "escape" a mechanistic imperative?

All existing assays of disulfide bond isomerization use protein substrates, such as bovine pancreatic ribonuclease (RNase A) (*39*) or bovine pancreatic trypsin inhibitor (BPTI) (*40*, *41*). RNase A is a 124-residue protein with four native disulfide bonds that are required for catalytic activity. Random oxidation of the 8 cysteine residues under denaturing conditions gives scrambled RNase A (sRNase A), a mixture of up to 105 ($=_8\mathbf{C}_8 \times 7 \times 5 \times 3$) distinct fully oxidized species, as well as numerous partially oxidized species.[3] BPTI contains only 6 cysteine residues but can still form 15 ($=_6\mathbf{C}_6 \times 5 \times 3$) fully oxidized species. The pathway of disulfide bond isomerization in a redox buffer is complicated further by a large number of potential mixed disulfide reaction intermediates (*42*). The heterogeneity of these protein substrates obfuscates mechanistic details.

Existing assays of disulfide reduction and dithiol oxidation often employ homogeneous peptide substrates (*43*). Such assays provide the opportunity for detailed mechanistic analyses of reduction and oxidation. Examples include a discontinuous assay based on chromatography (*44*) and continuous assays based on fluorescence (*45*−*50*) or luminescence (*51*). These assays invoke clever designs and have desirable attributes, including the possibility of monitoring intracellular reduction potentials (*51*). None, however, can be used to assay disulfide bond isomerization.

Here, we describe the design, synthesis, and use of a homogeneous substrate for a continuous assay of disulfide bond isomerization. We use this assay to analyze catalysis by wild-type PDI and active-site variants that lack one or the other of the active-site cysteine residues. The results provide new insight into the enzymatic catalysis of disulfide bond isomerization.

EXPERIMENTAL PROCEDURES

Materials. Escherichia coli strains BL21(DE3) and DH5α and the pET22b(+) expression vector were from Novagen (Madison, WI). DNA oligonucleotides for mutagenesis and sequencing were from Integrated DNA Technologies (Coralville, IA). Enzymes for DNA manipulation were from Promega (Madison, WI) and New England Biolabs (Beverly, MA). DNA-sequencing reactions were performed using the

[3] RNase A can form 764 ($=_8\mathbf{C}_8 \times 7 \times 5 \times 3 + {}_8\mathbf{C}_6 \times 5 \times 3 + {}_8\mathbf{C}_4 \times 3 + {}_8\mathbf{C}_2 + {}_8\mathbf{C}_0$) distinct oxidized, partially oxidized, and reduced species, altogether.

BigDye kit from Applied Biosystems (Foster City, IA) and CleanSeq magnetic beads from Agencourt Bioscience (Beverly, MA). DNA sequences were determined on an Applied Biosystems automated sequencing instrument at the University of Wisconsin Biotechnology Center. Poly(cytidylic acid) [poly(C)] was from Midland Certified Reagents (Midland, TX) and was precipitated from aqueous ethanol (70%, v/v) before use. Fluorenylmethoxycarbonyl (Fmoc)-protected amino acids were from Novabiochem (La Jolla, CA). Fmoc-Lys(dansyl)-OH was from AnaSpec (San Jose, CA). All other reagents were of reagent grade or better and were used without further purification.

Luria−Bertani (LB) medium contained (in 1.0 L) tryptone (10 g), yeast extract (5 g), and NaCl (10 g). Terrific broth (TB) medium contained (in 1.0 L) tryptone (12 g), yeast extract (24 g), glycerol (4 mL), K_2HPO_4 (72 mM), and KH_2PO_4 (17 mM). All media were prepared in deionized, distilled water and autoclaved.

Instrumentation. Measurements of UV and visible absorbance were made with either a Cary model 50 or a Cary model 3 spectrophotometer equipped with a Cary temperature controller (Varian, Palo Alto, CA). Peptide synthesis was conducted with a Pioneer automated synthesizer (PerCeptive Biosystems) at the University of Wisconsin Biotechnology Center. Preparative high-performance liquid chromatography (HPLC) was performed with a system from Waters (Milford, MA) equipped with two 510 pumps and a 486 tunable absorbance detector. Analytical HPLC was performed with a Waters system equipped with two 515 pumps, a 717 plus autosampler, and a 996 photodiode array detector. Fast protein liquid chromatography (FPLC) was performed with an ÄKTA system from Amersham Pharmacia (Piscataway, NJ). Fluorescence was measured with a QuantaMaster 1 photon-counting fluorescence spectrometer equipped with sample stirring (Photon Technology International, South Brunswick, NJ). Matrix-assisted laser desorption/ionization time-of-flight (MALDI−TOF) mass spectrometry was performed on a Perkin−Elmer (Wellesley, MA) Voyager MALDI−TOF mass spectrometer at the University of Wisconsin—Madison Biophysics Instrumentation Facility.

Design of a Substrate for a Disulfide Bond Isomerization Assay. We used tachyplesin I (TI) as a starting point for the development of a substrate for a disulfide bond isomerization assay. TI is a 17-residue antimicrobial peptide (Figure 2) that has been isolated from the hemocytes of the horseshoe crab, *Tachypleus tridentatus* (*52*). NMR structural analysis has revealed that the peptide folds into a β hairpin (*53*, *54*). Residues 3−8 and 11−16 define an antiparallel β sheet; residues Arg9 and Gly10 define a β turn; and the N- and C-terminal residues are disordered. The β sheet is stabilized by two disulfide bonds and six hydrogen bonds. The ability of TI to permeabilize membranes through the formation of anion-selective pores is attributed to an amphiphilic structure composed of a large number of hydrophobic and cationic residues (*54*−*56*). We suspected that the incorporation of a fluorescence donor−acceptor pair near the N and C termini of TI would enable us to monitor the acquisition of the native structure in a continuous manner by the appearance of FRET.

Synthesis of a Substrate for a Disulfide Bond Isomerization Assay. The synthesis of native TI (nTI) was performed using standard Fmoc-protection strategies. In nTI, the sequence of wild-type TI was altered slightly by capping the N terminus with an acetyl group, changing Lys1 to a glycine residue and Arg17 to a lysine residue, and replacing the C-terminal carboxamide with a glycine residue (Figure 2). All cysteine residues were protected with trityl (Trt) groups. Protected TI (approximately 0.1 mmol) was cleaved from the solid support, and its protecting groups were removed by treatment at room temperature for 1.5 h with a cocktail (5 mL) of trifluoroacetic acid (TFA, 82.5%, v/v), phenol (5%, v/v), thioanisole (5%, v/v), water (5%, v/v), and 2-ethanedithiol (EDT, 2.5%, v/v). The peptide was precipitated by dripping into cold diethyl ether (30 mL), collected by centrifugation, washed with diethyl ether (2 × 30 mL), and dried under vacuum.

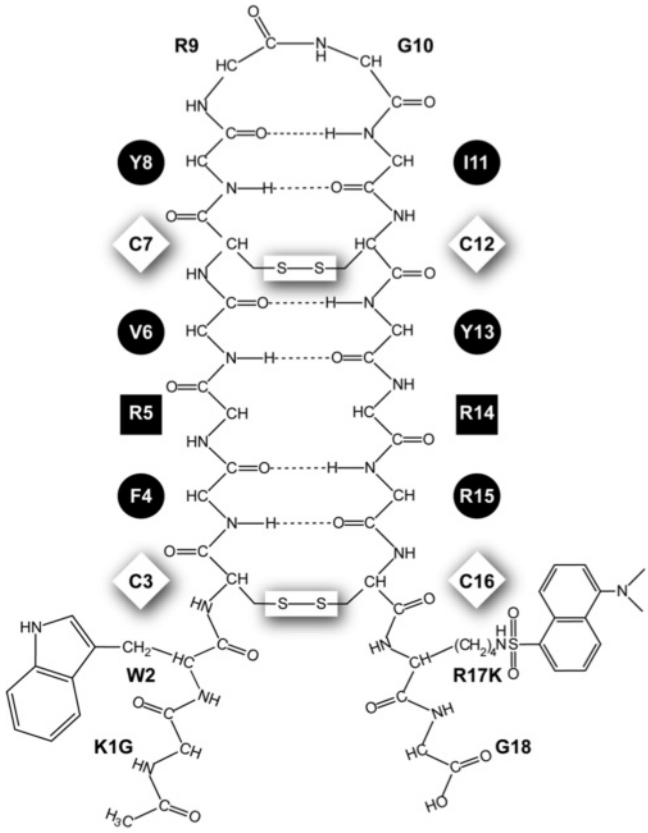

FIGURE 2: Structure of dns-nTI. Native TI is a β hairpin stabilized by six hydrogen bonds and two disulfide bonds (*53*, *54*). Side chains indicated with circles lie above the plane of the β sheet; side chains with squares lie below the plane of the β sheet. dns-nTI is identical to TI except with the N terminus acetylated, Lys1 replaced with a glycine residue, Arg17 replaced with a lysine residue, and the C-terminal carboxamide replaced with a glycine residue. The assay described herein relies on FRET from Trp2 to the dansyl group attached to Lys17.

Reduced TI was purified by reversed-phase HPLC using a Dynamax Microsorb preparative C18 column (21.4 × 250 mm), equipped with a guard column, from Varian (Lake Forest, CA). The peptide was eluted with a linear gradient (40 min) of aqueous acetonitrile (25−65%, v/v) containing TFA (0.1%, v/v) at a flow rate of 14.6 mL/min. Native disulfide bonds were formed by incubation with aqueous dimethyl sulfoxide (DMSO, 20%, v/v) overnight at room temperature. nTI was purified by HPLC as described above for reduced TI (MALDI−MS: $[M + H]^+$ calcd, 2265.0; found, 2265.8).

A dansyl (dns) group was attached to the ϵ-amino group of Lys17 of nTI. Oxidized nTI (7.0 mg, 1 mM) in DMF

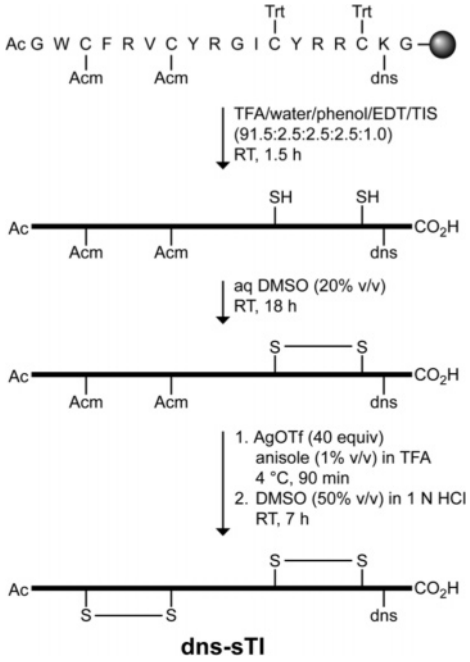

FIGURE 3: Scheme for the synthesis of dns-sTI. The peptide was synthesized on solid phase using standard Fmoc-protection methods. The lysine residue was protected with a dansyl (dns) group. The N-terminal cysteine residues were protected with acetamidomethyl (Acm) groups; the C-terminal cysteines were protected with trityl (Trt) groups. In the first step, the peptide was cleaved from the resin with the removal of all but the Acm-protecting groups. In the second step, the first disulfide bond was formed. In the final step, the Acm-protecting groups were removed and the second disulfide bond was formed.

(3.0 mL total) was stirred with DIEA (100 mM, 100 equiv) at 4 °C for 5 min prior to the addition of dansyl chloride (1 mM, 1 equiv). The reaction was allowed to proceed for 6 h at 4 °C. The reaction mixture was quenched by the addition of water (27 mL). Dansylated nTI (dns-nTI) was purified by HPLC on a preparative C18 column as described above for reduced nTI. Purified dns-nTI (5.0 mg, 2%) was dried under vacuum and analyzed by mass spectrometry (MALDI−MS: $[M + H]^+$ calcd, 2497.1; found, 2497.0).

Scrambled tachyplesin (sTI) contains the same amino acid sequence as does nTI, but the half-cystine pairings are nonnative. In sTI, Cys3 and Cys7 form one disulfide bond and Cys12 and Cys16 form a second disulfide bond. We chose these nonnative pairings (rather than Cys3−Cys12 and Cys7−Cys16) to mimic those that are most likely to arise during oxidative protein folding (*4*). These nonnative disulfide bonds were formed in solution through a pairwise protecting group strategy (Figure 3) (*57*). The synthesis of native TI (nTI) was performed using standard Fmoc-protection strategies. Cys3 and Cys7 were protected with acetamidomethyl (Acm) groups, while Cys12 and Cys16 were protected with trityl (Trt) groups. The N terminus of the peptide was capped with an acetyl group. Fmoc-Lys-(dansyl) was coupled as residue 17. Protected dns-sTI (approximately 0.1 mmol) was cleaved from the solid support, and its protecting groups [except Cys(Acm)] were removed by treatment at room temperature for 1.5 h with a cocktail (10 mL) of TFA (91.5%, v/v), phenol (2.5%, v/v), water (2.5%, v/v), EDT (2.5%, v/v), and triisopropylsilane (1.0%, v/v). dns-sTI(Acm) was precipitated by dripping into cold diethyl ether (30 mL), collected by centrifugation, washed with diethyl ether (2 × 30 mL), and dried under vacuum. Reduced dns-sTI(Acm) was purified by HPLC on a Dynamax Microsorb preparative C18 (21.4 × 250 mm) column, eluting with a linear gradient (30 min) of acetonitrile (30−60%, v/v, in water) containing TFA (0.1%, v/v).

The first nonnative disulfide bond (Cys12−Cys16) in dns-sTI(Acm) was formed by treatment with aqueous DMSO (20%, v/v) at room-temperature overnight. Oxidized dns-sTI(Acm) was purified by preparative HPLC as described above for reduced dns-sTI(Acm). Purified oxidized dns-sTI-(Acm) was dried by lyophilization and analyzed by mass spectrometry (MALDI−MS: $[M + H]^+$ calcd, 2641.2; found, 2640.9).

The second nonnative disulfide bond (Cys3−Cys7) in dns-sTI(Acm) was formed by the method of Fujii and co-workers (*58*−*60*). Specifically, the Acm groups were removed by treating the peptide (8 μmol) with silver trifluoromethanesulfonate (AgOTf, 50 equiv) in TFA (2 mL) containing anisole (1%, v/v) at 4 °C for 1.5 h. The peptide was precipitated in cold diethyl ether (5 mL), collected by centrifugation, and washed with cold diethyl ether (2 × 5 mL). Residual ether was removed under vacuum. The N-terminal disulfide bond was formed by oxidation with DMSO (50%, v/v) in 1 N HCl (4 mL) at room temperature for 7 h. Silver chloride was removed by filtration, and water was added (6 mL). The oxidized peptide (dns-sTI) was purified by HPLC on a Zorbax StableBond reversed-phase C8 column (9.4 × 250 mm) from Agilent (Wilmington, DE), eluting with a linear gradient (40 min) of acetonitrile (27−37%, v/v, in water) containing TFA (0.1%, v/v) at a flow rate of 4.1 mL/min. dns-nTI elutes at 31.1%, v/v, acetonitrile, while dns-sTI elutes at 31.7%, v/v, acetonitrile. The nonnative peptide (1.4 mg, 0.6%) was dried under vacuum; its purity (98%) was confirmed by analytical HPLC; and its identity was confirmed by mass spectrometry (MALDI−MS: $[M + H]^+$ calcd, 2497.1; found, 2497.4).

Handling of dns-nTI and dns-sTI. Fluorescence spectroscopy of dns-nTI and dns-sTI were complicated by their adsorption to typical cuvettes. This adsorption was lessened by the use of methacrylate cuvettes (4.5 mL, 1 × 1 cm, Fisher Scientific, Pittsburgh, PA). In addition, cuvettes and stir bars were soaked in aqueous poly(ethylenimine) (1%, w/v) for at least 1 h and then rinsed with deionized, distilled water prior to their use. Buffers were supplemented with the detergent IGEPAL CA-630 (0.01%, w/v) to reduce peptide adsorption further.

Physical Characterization of dns-nTI and dns-sTI. The molar extinction coefficient of dns-nTI was determined at 280 nm by using the method of Gill and von Hippel (*61*) and a value of $\epsilon_{280} = 4141\ M^{-1}\ cm^{-1}$ for the dansyl group determined with dansyl glycine (Sigma Chemical) and Beer's law. The resulting value of $\epsilon_{280} = 10\,680\ M^{-1}\ cm^{-1}$ was used to calculate concentrations of dns-nTI and dns-sTI in purified samples.

The half-cystine pairings in dns-nTI and dns-sTI were confirmed by proteolytic digestion with α-chymotrypsin. Peptide (15 μg) was incubated at 37 °C for 18 h with α-chymotrypsin (0.5 μg) in 100 mM Tris-HCl buffer at pH 7.6, containing $CaCl_2$ (1 mM). Digested fragments were isolated by analytical HPLC on a reversed-phase C18 column (4.8 × 250 mm) from Varian and were identified by mass spectrometry. On the basis of preliminary work with non-

fluorescent nTI and sTI, we were aware of some unusual digestion patterns for TI. First, α-chymotrypsin cleaves both peptides after the consecutive arginine residues at positions 14 and 15. A similar response of α-chymotrypsin to consecutive arginine residues had been observed previously (*62*). In addition, α-chymotrypsin is unable to cleave after Phe4 in sTI. This residue is within the loop defined by the Cys3−Cys7 disulfide bond, which could hinder access. Given these observations, digestion of the purified peptides and analysis by mass spectrometry yielded fragments diagnostic of dns-nTI (MALDI−MS: $[M + H]^+$ calcd, 806.3 and 1148.5; found, 806.5 and 1148.9) and dns-sTI (MALDI−MS: $[M + H]^+$ calcd, 788.3 and 1148.5; found, 789.0 and 1149.3).

Disulfide Bond Reduction Potential of dns-nTI. The reduction potential of dns-nTI was determined by using fluorescence spectroscopy to characterize thiol−disulfide exchange equilibria established between dns-nTI and glutathione. Reaction buffer (which was 100 mM Tris-HCl buffer at pH 7.6, containing 1 mM EDTA and 0.01%, w/v, IGEPAL CA-630) containing various ratios of reduced/oxidized glutathione [$E^{\circ\prime} = -0.252$ V (*63*)] was degassed for 30 min and flushed with argon for ≥40 min. The peptide (480 nM) was then added to the deoxygenated buffer, and the fluorescence emission at 465 nm upon excitation at 280 nm was recorded once equilibrium had been attained (20 min). The fluorescence emission at equilibrium was plotted as a function of the reduction potential of the buffer. The standard reduction potential of dns-nTI was calculated by nonlinear least-squares analysis of the data with the Nernst equation:

$$F = F_0 + \frac{F_{max} - F_0}{1 + e^{-(E-E^\circ)(n\mathcal{F}RT)}} \quad (1)$$

where n is the number of electrons, $\mathcal{F}$ is the Faraday constant (96 494 J V^{-1} mol^{-1}), R is the gas constant (8.314 J K^{-1} mol^{-1}), T is the temperature (here, 298 K), E is the reduction potential of the solution, and E° is the reduction potential of dns-nTI. To investigate cooperativity between the two disulfide bonds, the data were depicted in a Hill plot, which here is a log plot of the ratio of reduced to oxidized peptide (determined by relative fluorescence emission) as a function of $[GSH]^2/[GSSG]$. The Hill coefficient of cooperativity (h) and a confirmation of the value of E° for dns-nTI were calculated by nonlinear least-squares analysis of the data with the equation

$$\log([\text{dns-rTI}]/[\text{dns-nTI}]) = h \log([GSH]^2/[GSSG]) - \log(K_{eq}) \quad (2)$$

where K_{eq} is the equilibrium constant between dns-nTI and dns-rTI as mediated by glutathione.

Plasmid for Production of Human PDI and Its Variants. A plasmid containing the human PDI cDNA was a generous gift from Alan D. Attie (University of Wisconsin−Madison). This plasmid contains the cDNA for a variant of human PDI with two SGHC active sites (hPDIx) inserted between the *Bgl*II and *Bam*HI sites of the pET22b(+) vector. The hPDIx cDNA was isolated by restriction digest and inserted into the *Bam*HI site of pBK1 [a pET22b(+) vector in which the *Eco*RI site had been removed] to give pBK1·hPDIx1. Two unique restriction sites, *Eco*RI, 5′ to the first active site, and *Mfe*I, 3′ to the second active site, were added to the PDI cDNA by using the Kunkel method of mutagenesis to give pBK1·hPDIx4 (*64*). A unique *Nde*I site was added at the 5′ end of the coding region of the cDNA, placing an ATG start codon in place of the final codon of the signal sequence coding region. Restriction digest with *Nde*I and *Bam*HI, followed by ligation, removed the 5′ signal-sequence coding region to give pBK1·hPDIx6, which is a vector for the production of SGHC/SGHC PDI (in which both active sites have a SGHC sequence).

A vector for the production of wild-type human PDI was obtained by PCR mutagenesis with two primers, one complementary to the 5′ active-site region, including the *Eco*RI restriction site (GTGGAATTCTATGCTCCTTGGTGCGGCCACTG), and one complementary to the 3′ active-site region, including the *Mfe*I restriction site (GGGAGCCAATTGTTTGCAGTGACCACACCATGG). The PCR product was cloned into the PCR4-TOPO cloning vector (Invitrogen, Carlsbad, CA) and confirmed by DNA sequencing. Digestion with *Eco*RI and *Mfe*I followed by ligation yielded plasmid pBK1·PDI1, which directs the expression of wild-type human PDI.

A vector for the production of CGHA/CGHA PDI (in which both active sites have a CGHA sequence) was obtained in a series of steps. First, QuikChange (Stratagene, La Jolla, CA) site-directed mutagenesis was used to change the second cysteine codon of the N-terminal active site to one for alanine (GCT). The Kunkel method of mutagenesis was then used to change the second cysteine codon of the C-terminal active site to one for alanine (GCT). The resulting plasmid pBK1·PDI2 directs the expression of human PDI with two CGHA active sites.

Production and Purification of Human PDI and Its Variants. A plasmid encoding human PDI or a variant was transformed by electroporation into *E. coli* strain BL21(DE3), which was then grown on LB agar containing ampicillin (200 μg/mL). A starter culture in LB medium (25 mL) containing ampicillin (200 μg/mL) was inoculated with a single colony and then shaken overnight at 37 °C. TB medium (1.0 L) containing ampicillin (200 μg/mL) was inoculated with a starter culture to OD = 0.01 at 600 nm and then shaken (210 rpm) at 37 °C until reaching OD = 1.7−2.0 at 600 nm. Protein expression was induced by the addition of IPTG (0.5 mM) and shaking for an additional 4 h at 37 °C.

Cells (10 g of wet weight) were harvested by centrifugation and resuspended in 15 mL of 50 mM Tris-HCl buffer at pH 8.0, containing EDTA (2 mM). Cells were lysed by passage (3×) through a French pressure cell. Insoluble material was removed by ultracentrifugation at 50000*g* for 1 h at 4 °C. The lysate was clarified further by an ammonium sulfate fractionation. Specifically, saturated ammonium sulfate was added to the lysate to 55% saturation, and the pellet was removed by centrifugation at 15000*g* for 30 min. The supernatant was precipitated by adding saturated ammonium sulfate to 85% saturation. The pellet was isolated by centrifugation at 15000*g* for 30 min and resuspended in 25 mM sodium phosphate buffer at pH 8.0, containing NaCl (0.40 M). The 55−85% ammonium sulfate fraction was dialyzed overnight against 4.0 L of the same buffer.

The dialyzed lysate was loaded onto Hi Load 26/60 Superdex-200 gel-filtration FPLC resin (Amersham Bio-

sciences) that had been pre-equilibrated with 25 mM sodium phosphate buffer at pH 8.0, containing NaCl (0.40 M). The resin was eluted with the same buffer at a flow rate of 2.0 mL/min. Fractions containing PDI were identified by SDS−PAGE analysis and pooled. The elution of PDI from the gel-filtration column was indicative of a protein of 58 kDa based on a calibration curve obtained with a calibration kit (29−700 kDa) from Sigma Chemical (St. Louis, MO). Fractions containing PDI were combined and dialyzed overnight against 4.0 L of 25 mM sodium phosphate buffer at pH 6.8.

Dialyzed protein from gel-filtration chromatography was injected at 2 mL/min onto 8 mL of Resource Q anion-exchange FPLC resin (Amersham Biosciences) that had been pre-equilibrated with 25 mM sodium phosphate buffer at pH 6.8. After washing with 24 mL of equilibration buffer, PDI was eluted with a linear gradient (90 + 90 mL) of NaCl (0−1.00 M) in equilibration buffer. Fractions containing PDI, which eluted at approximately 0.32 M NaCl, were combined and dialyzed overnight against 4.0 L of 25 mM sodium phosphate buffer at pH 6.0. After dialysis, purified protein was concentrated to approximately 1.0 mg/mL using a Vivaspin concentrator (20 mL; molecular mass cutoff, 10 kDa; Vivascience AG, Hanover, Germany) and stored at −80 °C. Typically, 10 mg of PDI (>95% pure) was obtained from a 1-L growth.

Disulfide Bond Isomerization Assay with dns-sTI. Assays were performed in a volume of 2.0 mL at room temperature. Excitation and emission slit widths were both 4 nm. The reaction buffer was degassed under vacuum for 30 min and flushed with argon for 40 min to minimize air oxidation. Prior to each assay, the dns-sTI substrate (1.1 μM) was incubated in deoxygenated reaction buffer for 1 min and its initial fluorescence (F_0) was recorded. PDI was preincubated with glutathione (116 μM GSH and 4 μM GSSG) in deoxygenated reaction buffer at room temperature for 30 min. To initiate the isomerization reaction, GSH (116 μM), GSSG (4 μM), and pre-equilibrated PDI (10−50 nM) were added simultaneously to the solution of the substrate. Isomerization was measured as a function of time by monitoring the increase in fluorescence emission at 465 nm upon excitation at 280 nm. A typical data set is shown in Figure 4B.

Kinetic parameters were determined with nonlinear least-squares regression analysis with the equation

$$F = F_0 - (F_{max} - F_0)(1 - e^{-kt}) \quad (3)$$

where F refers to the fluorescence emission at known times and F_{max} refers to the fluorescence emission of dns-nTI. dns-sTI concentrations of ≤16 μM did not saturate the enzyme (data not shown). Accordingly, the first-order rate constant k in eq 3 is equivalent to $(k_{cat}/K_M)[E]$ after correction for any uncatalyzed reaction.

Disulfide Bond Isomerization Assays with sRNase A. sRNase A was prepared by air oxidation of reduced RNase A (~35 μM) over several days in 100 mM Tris-HCl buffer at pH 8.0, containing guanidine-HCl (6.0 M) and EDTA (1.0 mM). The protein was then dialyzed against 100 mM Tris-HCl buffer at pH 7.6, containing EDTA (1.0 mM). This process produced RNase A that contained <0.1 mol of thiol/mol of protein.

The isomerization of sRNase A to form native RNase A was measured essentially as described previously (*65*, *66*).

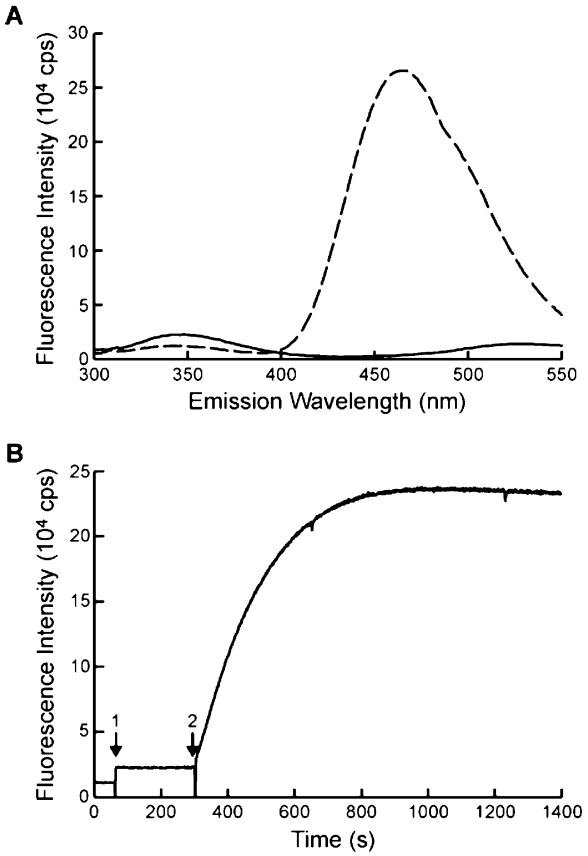

FIGURE 4: Fluoresence properties of dns-nTI and dns-sTI. (A) Fluorescence emission intensity of dns-nTI (1.1 μM, - - -) and dns-sTI (1.1 μM, —) as a function of the wavelength upon excitation at 280 nm. Emission intensity was corrected for that of the buffer (100 mM Tris-HCl buffer at pH 7.6, containing 1 mM EDTA). (B) Fluorescence emission intensity (emission at 465 nm and excitation at 280 nm) of dns-sTI (1.1 μM) as a function of time after the addition of PDI (20 nM) and glutathione (116 μM GSH and 4 μM GSSG). The reaction was performed in 100 mM Tris-HCl buffer at pH 7.6, containing EDTA (1 mM) and IGEPAL CA-630 (0.01%, w/v). dns-sTI was added at time point 1; PDI and glutathione were added at time point 2.

To prevent air oxidation, reaction buffer [which was 100 mM Tris-HCl buffer at pH 7.6, containing EDTA (1 mM)] was degassed under vacuum for 30 min and flushed with argon for 30 min. Assays were performed under a positive pressure of argon at 23 °C in a reaction buffer (1.0 mL) containing GSH (1.0 mM), GSSG (0.2 mM), and PDI (360 nM). The reaction was initiated by addition of sRNase A (3.6 μM). Aliquots (50 μL) were removed and quenched with acetic acid (5 μL, 10%, v/v) at timed intervals. These aliquots were assayed for poly(C)-cleavage activity by monitoring the change in absorbance at 238 nm. Data were fitted to an exponential curve to obtain second-order rate constants. Specific activity was calculated from the difference in rate constants for the catalyzed and uncatalyzed reactions.

RESULTS

Design and Synthesis of Substrate for a Disulfide Bond Isomerization Assay. We reasoned that an ideal substrate for a disulfide bond isomerization assay should have the following attributes. The substrate should have four cysteine residues, which would allow for three possible fully oxidized species. One of these oxidized species should be the most

stable and therefore "native". To be a substrate for isomerization, the disulfide bonds in the native conformation should have a reduction potential ($E^{\circ\prime}$) that is more negative (i.e., indicative of a more stable disulfide bond) than the reduction potential of the PDI active sites [$E^{\circ\prime} = -0.180$ V (*67*)]. Otherwise, PDI would merely catalyze the reduction of the disulfide bonds in the substrate. Finally, structural changes accompanying native disulfide bond formation should be perceivable in a continuous manner.

TI, which is a natural 17-residue peptide, was used as the basis for a continuous assay of disulfide bond isomerization. The small size of this peptide allowed for its synthesis by standard solid-phase methods. The assay relied on FRET from Trp2 to an installed dansyl group. The Trp-dansyl interaction has a small Förster radius [approximately 20 Å (*68*)] and is known to provide a sensitive measure of short distances within peptides and proteins of flexible conformation (*68*−*71*). This FRET pair enabled us to distinguish readily between the native β-hairpin species (dns-nTI), in which the peptide termini are close together, and a nonnative species (dns-sTI), in which the termini are far apart. Preliminary investigation of numerous alternative FRET donor−acceptor pairs did not give adequate sensitivity (data not shown).

A few changes were made to the amino acid sequence of TI to allow for the site-specific placement of a FRET pair (Figure 2). These changes were made at the N and C termini of the peptide, which are mobile in solution (*53*, *54*) and thus unlikely to compromise β-hairpin stability. Our design called for a dansyl group to be attached to the ϵ-amino group of a lysine residue installed at position 17 in place of the arginine residue in wild-type TI. To make the ϵ-amino group of Lys17 uniquely available for N-dansylation, we replaced Lys1 with a glycine residue and acetylated the N terminus. Finally, we replaced the C-terminal carboxamide with a glycine residue to facilitate peptide synthesis.

The synthesis of nonnative disulfide bonds was achieved by a pairwise protecting group strategy (*57*) in which the two N-terminal cysteine residues were Acm-protected during peptide synthesis, while the two C-terminal cysteine residues were Trt-protected (Figure 3). The acid-labile Trt groups were removed during cleavage from the resin, and the C-terminal cysteine residues were oxidized by aqueous DMSO. Under these conditions, the Acm groups remain intact, as confirmed by mass spectrometry. In the final step of dns-sTI synthesis, the Acm groups were removed using AgOTf and the N-terminal cysteine residues were oxidized in DMSO/aqueous HCl (*58*−*60*). Other oxidation methods, including silyl chloride/diphenylsulfoxide (*72*, *73*) and TFA/DMSO (*74*) as well as iodine oxidation (*75*, *76*), were unsuccessful because of modification and decomposition of Trp2. The nonnative conformation comprised 42% of the peptide product after oxidation by the AgOTf/DMSO/aqueous HCl method, with 58% being in the native conformation as measured by the integration of HPLC peaks. The overall yield for the synthesis of dns-sTI was nearly 1% (1.4 mg from a 100-μmol scale synthesis), while the overall yield for the synthesis of dns-nTI, which did not require a pairwise cysteine protection but did involve the solution-phase addition of a dansyl group, was 2% (5.0 mg from a 100-μmol scale synthesis).

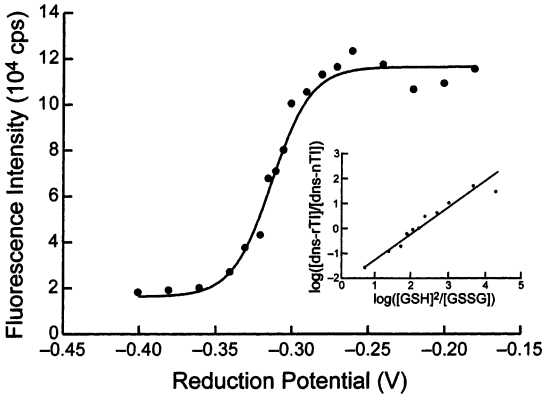

FIGURE 5: Fluorescence emission intensity (emission at 465 nm and excitation at 280 nm) of dns-nTI as a function of the solution reduction potential. Thiol−disulfide exchange equilibria were established between dns-nTI (465 nM) and varying ratios of reduced to oxidized glutathione for 20 min prior to the measurement of fluorescence. The reduction potential of dns-nTI ($E^\circ = -0.313$ V) was obtained by nonlinear least-squares analysis of the data with eq 1 and $n = 2$. Linear least-squares analysis of the data in a Hill plot (inset) indicated no cooperativity ($h = 1.018$ and $E^\circ = -0.314$ V).

Fluorescence Properties of dns-nTI and dns-sTI. In 100 mM Tris-HCl buffer at pH 7.6, containing EDTA (1 mM), dns-nTI (1.1 μM) had a maximal fluorescence emission at 465 nm upon excitation at 280 nm because of FRET between Trp2 and dansyl (Figure 4A). The same concentration of dns-sTI had a fluorescence emission spectrum that did not indicate significant fluorescence emission at 465 nm but instead displayed fluorescence emission from Trp2 at 340 nm (Figure 4A). The conversion from the nonnative to the native disulfide conformation was accompanied by a substantial increase in fluorescence emission at 465 nm, with $F_{max}/F_0 = 28 \pm 2$ after correcting for buffer fluorescence (Figure 4B). Replicate synthetic preparations of dns-nTI and dns-sTI had spectroscopic parameters that did not differ significantly.

Reduction Potential of dns-nTI. The reduction potential (E°) of a disulfide bond is a measure of its stability. We measured the reduction potential of dns-nTI upon equilibration in buffers containing various ratios of reduced to oxidized glutathione. The fluorescence emission intensity obtained in these different redox buffers indicated the amount of oxidized versus reduced peptide (Figure 5). Nonlinear least-squares analysis of the data with eq 1 and $n = 2$ gives $E^\circ = -0.313$ V ($r^2 = 0.990$) for dns-nTI. This value actually reported on the disappearance of FRET upon the reduction of one disulfide bond in dns-nTI. It is likely, however, that the second disulfide bond has $E^\circ > -0.313$ V and is thus reduced readily in solutions with $E \leq -0.313$ V. Indeed, a Hill plot of the data (inset of Figure 5) gives $h = 1.018$, suggesting that there was no significant cooperativity in the reduction of the two disulfide bonds. In addition, the value of $E^\circ = -0.314$ V obtained with eq 2 is in gratifying agreement with that obtained with eq 1.

Isomerization of dns-sTI by PDI. Disulfide bond isomerization in the presence of substoichiometric amounts of PDI was assayed by monitoring the increase in fluorescence emission at 465 nm upon excitation at 280 nm over time. In reaction buffer alone (no catalyst or redox buffer), the fluorescence emission of dns-sTI did not change over the

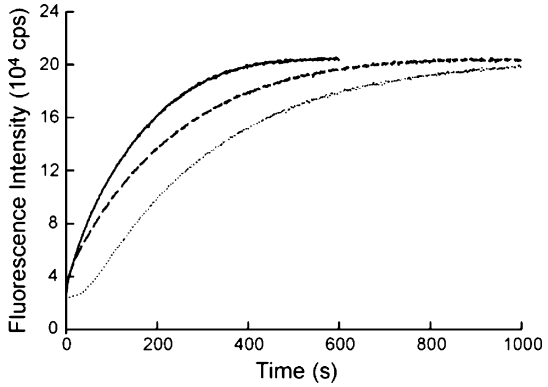

FIGURE 6: Typical assay of the isomerization of dns-sTI. Fluorescence emission intensity (emission at 465 nm and excitation at 280 nm) of dns-sTI (1.1 μM) was monitored after the addition of wild-type human PDI (20 nM, —), CGHA/CGHA PDI (20 nM, - - -), or glutathione alone (•••). Reactions were performed in 100 mM Tris-HCl buffer at pH 7.6, containing EDTA (1 mM), IGEPAL CA-630 (0.01%, w/v), and glutathione (116 μM GSH and 4 μM GSSG).

Table 1: Catalysis of Disulfide Bond Isomerization by Protein Disulfide Isomerase

active sites	k_{cat}/K_M for dns-sTI (10^5 M^{-1} s^{-1})	k_{cat}/K_M for dns-sTI (%)	specific activity for sRNaseA (units/μmol)[a]	specific activity for sRNaseA (%)
CGHC/CGHC	1.7 ± 0.5	100	360 ± 69	100
CGHA/CGHA	0.86 ± 0.35	51	28 ± 18	7.7
SGHC/SGHC	nd[b]	nd[b]	0.56 ± 0.83	0.16

[a] A total of 1 unit catalyzes the activation of 1 nmol of sRNase A/min in 100 mM Tris-HCl buffer at pH 7.6, containing EDTA (1.0 mM), GSH (1.0 mM), and GSSG (0.2 mM). [b] nd = not determined.

time course of the assay (30 min, data not shown). The presence of glutathione (116 μM GSH and 4 μM GSSG) in the assay buffer ensured that PDI was maintained in an optimum redox state.[4] In the absence of the enzyme, glutathione alone can catalyze the conversion of dns-sTI to dns-nTI (Figure 6). At the concentrations used here, isomerization by glutathione shows a delay of approximately 20 s. The rate constant for the nonenzymatic reaction was calculated by fitting the curve following the lag to eq 3.

In the presence of wild-type PDI (20 nM), the conversion of dns-sTI to dns-nTI was nearly complete within approximately 7 min, as observed by the fluorescence emission intensity (Figure 6). In the presence of increasing concentrations of enzyme, the first-order rate constant increased as expected (data not shown). Data from triplicate reactions and at varying concentrations of wild-type PDI yielded a k_{cat}/K_M value of $(1.7 \pm 0.5) \times 10^5$ M^{-1} s^{-1} (Table 1). The k_{cat}/K_M value of the CGHA/CGHA variant was $(0.86 \pm 0.35) \times 10^5$ M^{-1} s^{-1}, approximately half that of the wild-type enzyme (Table 1).

Isomerization of sRNase A by PDI. The traditional assay for disulfide bond isomerization measures the increase in ribonucleolytic activity upon the addition of catalyst to sRNase A. In the presence of substoichiometric amounts of wild-type PDI (360 nM), sRNase A (3.6 μM) is converted to active RNase A within approximately 2 h. The yield of native protein is, on average, only 50%. Data from triplicate reactions were fitted to an exponential rate curve and corrected for the uncatalyzed reaction to give a specific activity of 360 ± 69 nmol of sRNase reactivated min^{-1} μmol^{-1} (Table 1). Isomerization of sRNase A by CGHA/CGHA PDI was less efficient, having a specific activity of 28 ± 18 nmol min^{-1} μmol^{-1}. SGHC/SGHC PDI had no significant activity above the glutathione background (specific activity = 0.56 ± 0.83 nmol min^{-1} μmol^{-1}).

DISCUSSION

Despite decades of research, our understanding of the mechanism by which PDI catalyzes disulfide bond isomerization of disulfide bonds in proteins is far from complete. The role of the N-terminal active-site thiolate in the initial attack of a nonnative substrate disulfide has been well-established (*44*, *77*). Yet, it is still unclear how PDI initially recognizes its substrate. The C-terminal active-site cysteine residue appears to be involved in the rescue of trapped mixed disulfide intermediates during catalysis of sRNase A isomerization (*36*). However, this residue is not required for complementation of *pdi1*Δ *S. cerevisiae* (*28*). More detailed chemical analyses of the mechanism of isomerization are required for a complete understanding of the pathway of native disulfide bond formation. These analyses cannot be performed with heterogeneous substrates.

We have addressed the need for a homogeneous substrate for disulfide bond isomerization assays. When the sequence of tachyplesin I was adapted to incorporate donor and acceptor fluorophores, we were able to use FRET to follow the rearrangement from nonnative to native disulfide bonds directly and continuously. The Trp-dansyl pair is an ideal choice for this assay. Its small Förster radius allows us to observe the small distance changes that accompany the conversion of substrate to product, which likely involves a small change in the donor−acceptor distance. Indeed, the observed 28-fold increase in fluorescence emission that accompanies the conversion of dns-sTI to dns-nTI (Figure 4) is much larger than fluorescence changes observed in existing assays of disulfide reduction and dithiol oxidation (*45*−*50*).

The disulfide bond isomerization assay described herein has a number of advantages over the most common assay, in which sRNase A is the substrate. dns-sTI is a single, well-defined substrate. In contrast, sRNase A is a random mixture of innumerable fully and partially oxidized species. The complexity of the sRNase A substrate means that some folding intermediates will be unproductive, even in the presence of PDI. Thus, in a typical assay with sRNase A, only 50% of the substrate is converted to native protein. Using a small peptide substrate, conformational traps are avoided and dns-sTI is converted completely to dns-nTI, simplifying kinetic analyses. The isomerization of sRNase A by wild-type PDI takes 2 h to run to completion and is monitored indirectly by the appearance of ribonucleolytic activity. The isomerization of dns-sTI, on the other hand, is complete within 7 min and is monitored directly by FRET. Finally, the assay with dns-sTI requires a small amount of

[4] Although air oxidation was minimized by deoxygenating all solutions prior to performing assays, the fluorescence spectrometer was not equipped for operation under oxygen-free conditions. Hence, attempts to use reduced PDI as a catalyst in the absence of a redox buffer were unsuccessful because of the air oxidation of PDI prior to complete isomerization of dns-sTI.

enzyme (20 nM) for accurate and sensitive kinetic measurements, while the assay with sRNase A usually employs significantly higher concentrations of PDI (≥360 nM).

In the design of a disulfide bond isomerization assay, it is essential that PDI catalyzes rearrangement of nonnative disulfides in the substrate peptide but does not reduce native disulfides in the product peptide. Accordingly, a challenge in the search for an ideal substrate is to identify a peptide with an appropriate reduction potential for isomerization by PDI. The reduction potential determined here of $E^\circ = -0.313$ V confirms that dns-nTI is a poor substrate for reduction by PDI [$E^{\circ\prime} = -0.180$ V (*67*)]. This reduction potential also indicates that dns-nTI could be reduced by dithiothreitol [$E^{\circ\prime} = -0.330$ V (*78*)] but not by thioredoxin [$E^{\circ\prime} = -0.270$ V (*79*)], the ubiquitous cellular reductant.

The value of k_{cat}/K_M for the isomerization of dns-sTI by human PDI is 1.7×10^5 M^{-1} s^{-1} (Table 1). This value is the largest reported for catalysis of disulfide bond isomerization by PDI or any catalyst. This high catalytic efficiency likely arises from two factors. First, dns-sTI is a simple substrate with solvent-accessible disulfide bonds. Even a glutathione redox buffer can catalyze its turnover at a measurable rate (Figure 6). In contrast, complex substrates that can form unproductive intermediates along their folding pathway typically display larger rate enhancements with PDI (*80*). Second, nTI is a stable product ($E^\circ = -0.313$ V) that provides a thermodynamic imperative for substrate turnover.

The isomerization of dns-sTI is mediated by a glutathione redox buffer alone. The first seconds of the reaction display unusual behavior for an isomerization assay, with a lag in product formation preceding a steady-state phase. The length of the lag decreases with increasing concentrations of glutathione (data not shown) and is approximately 20 s in the assays performed herein (Figure 6). A similar lag is observed in oxidative folding assays that use reduced RNase A as the substrate and has been attributed to a slow initial oxidation step in which nonnative disulfide intermediates accumulate (*29*, *81*). In the dns-sTI assay, the lag could likewise report on the slow formation of mixed disulfide intermediates between glutathione and dns-sTI. The nucleophilic attack of reduced glutathione on disulfide bonds is inefficient at pH 7.6 because of its high thiol pK_a of 9.0 (*66*, *82*). In the presence of the enzyme, the lag phase is not observed because mixed disulfide formation by PDI is significantly more efficient because of its low active-site thiol pK_a of 6.7 (*77*).

We have used the dns-sTI substrate to investigate the role of the more C-terminal cysteine residue of the PDI active site in the mechanism of isomerization. Previous studies have revealed that variants of PDI in which the C-terminal cysteine is replaced with serine or alanine are less effective catalysts for the isomerization of sRNase A (*29*, *36*, *83*). This finding has been confirmed in the current study. CGHA/CGHA PDI displays a specific activity that is only 7.7% of wild-type PDI for the isomerization of sRNase A (Table 1). As predicted, mutation of the N-terminal cysteine residue to serine (as in SGHC/SGHC PDI) destroys all isomerase activity. The relative isomerase activity of CGHA/CGHA PDI in this study is slightly lower than values obtained in other studies using sRNase A as the substrate (*29*, *36*), with the discrepancy typifying the intrinsic variability of the sRNase A assay. Still, our data support the hypothesis that the C-terminal cysteine residue is important for the rescue of trapped mixed disulfide intermediates that accumulate during the oxidative folding of a complex substrate protein (*29*, *36*, *37*).

The isomerization of dns-sTI by CGHA/CGHA PDI is also less efficient than that catalyzed by the wild-type enzyme. For this substrate, however, the variant retains 51% of the activity of wild-type PDI. The replacement of the C-terminal cysteine residue with alanine is known to diminish by ca. 50% the intrinsic reactivity of the N-terminal cysteine residues in the PDI active sites toward oxidized glutathione, perhaps by increasing the pK_a of those cysteine residues (*84*). The lower rate of isomerization of dns-sTI by CGHA/CGHA PDI is in complete accordance with its lower intrinsic reactivity and indicates that the C-terminal cysteine residues in the PDI active sites do not play a significant role in the isomerization of dns-sTI.

CONCLUSIONS

The work described herein provides a new tool for studying the catalytic mechanism of disulfide bond isomerization. Unlike traditional isomerization assays, the assay uses a homogeneous substrate and is continuous. The substrate is completely converted to product in minutes using nanomolar concentrations of PDI. Kinetic analysis using the dns-sTI substrate and the CGHA/CGHA variant of PDI has increased our understanding of the catalytic mechanism of disulfide bond isomerization. The rate of sRNase A folding is substantially lower in the absence of the C-terminal cysteine residues in the PDI active sites. In contrast, the rate of dns-sTI folding is only moderately lower, as expected from the intrinsic decrease in the reactivity of the N-terminal cysteine residues in CGHA/CGHA PDI. These results suggest that the escape mechanism (Figure 1) does not contribute significantly to the folding of simple substrates. We anticipate that our approach will be useful for additional mechanistic studies of PDI, as well as its variants, homologues, and small-molecule mimics.

ACKNOWLEDGMENT

We thank Dr. G. L. Case and the Peptide Synthesis Facility at the University of Wisconsin—Madison for technical assistance and Prof. A. D. Attie for the cDNA of human PDI. We are grateful to Dr. K. J. Woycechowsky for valuable discussions.

REFERENCES

1. Thornton, J. M. (1981) Disulphide bridges in globular proteins, *J. Mol. Biol. 151*, 261−287.
2. Darby, N., and Creighton, T. E. (1995) Disulfide bonds in protein folding and stability, *Methods Mol. Biol. 40*, 219−252.
3. Yano, H., Kuroda, S., and Buchanan, B. B. (2002) Disulfide proteome in the analysis of protein structure and function, *Proteomics 2*, 1090−1096.
4. Welker, E., Wedemeyer, W. J., Narayan, M., and Scheraga, H. A. (2001) Coupling of conformational folding and disulfide-bond reactions in oxidative folding of proteins, *Biochemistry 40*, 9059−9064.
5. Flory, P. J. (1969) *Statistical Mechanics of Chain Molecules*, Wiley, New York.
6. Raines, R. T. (1997) Nature's transitory covalent bond, *Nat. Struct. Biol. 4*, 424−427.

7. Zhang, R., and Snyder, G. H. (1989) Dependence of formation of small disulfide loops in two-cysteine peptides on the number and types of intervening amino acids, *J. Biol. Chem. 264*, 18472−18479.
8. Freedman, R. B., Hirst, T. R., and Tuite, M. F. (1994) Protein disulphide isomerase: Building bridges in protein folding, *Trends Biochem. Sci. 19*, 331−336.
9. Guzman, N. A., Ed. (1998) *Prolyl Hydroxylase, Protein Disulfide Isomerase, and Other Structurally Related Proteins*, Marcel Dekker, New York.
10. Noiva, R. (1999) Protein disulfide isomerase: The multifunctional redox chaperone of the endoplasmic reticulum, *Semin. Cell Dev. Biol. 10*, 481−493.
11. Kersteen, E. A., and Raines, R. T. (2003) Catalysis of protein folding by protein disulfide isomerase and small-molecule mimics, *Antioxid. Redox Signaling 5*, 413−424.
12. Wilkinson, B., and Gilbert, H. F. (2004) Protein disulfide isomerase, *Biochim. Biophys. Acta 1699*, 35−44.
13. Ellgaard, L., and Ruddock, L. W. (2005) The human protein disulphide isomerase family: Substrate interactions and functional properties, *EMBO Rep. 6*, 28−32.
14. Edman, J. C., Ellis, L., Blacher, R. W., Roth, R. A., and Rutter, W. J. (1985) Sequence of protein disulphide isomerase and implications of its relationship to thioredoxin, *Nature 317*, 267−270.
15. Kemmink, J., Darby, N. J., Dijkstra, K., Nilges, M., and Creighton, T. E. (1997) The folding catalyst protein disulfide isomerase is constructed of active and inactive thioredoxin modules, *Curr. Biol. 7*, 239−245.
16. Darby, N. J., van Straaten, M., Penka, E., Vincentelli, R., and Kemmink, J. (1999) Identifying and characterizing a second structural domain of protein disulfide isomerase, *FEBS Lett. 448*, 167−172.
17. Koivunen, P., Salo, K. E. H., Myllyharju, J., and Ruddock, L. W. (2005) Three binding sites in protein disulfide isomerase cooperate in collagen prolyl 4-hydroxylase tetramer assembly, *J. Biol. Chem. 280*, 5227−5235.
18. Klappa, P., Ruddock, L. W., Darby, N. J., and Freedman, R. B. (1998) The b2 domain provides the principal peptide-binding site of protein disulfide isomerase but all domains contribute to binding misfolded proteins, *EMBO J. 17*, 927−935.
19. Cheung, P. Y., and Churchich, J. E. (1999) Recognition of protein substrates by protein-disulfide isomerase, *J. Biol. Chem. 274*, 32757−32761.
20. Munro, S., and Pelham, H. R. B. (1987) A C-terminal signal prevents secretion of luminal ER proteins, *Cell 48*, 899−907.
21. Farquhar, R., Honey, H., Murant, S. J., Bossier, P., Schultz, L., Montgomery, D., Ellis, R. W., Freedman, R. B., and Tuite, M. F. (1991) Protein disulfide isomerase is essential for viability in *Saccharomyces cerevisiae*, *Gene 108*, 81−89.
22. LaMantia, M., Miura, T., Tachikawa, H., Kaplan, H. W., Lennarz, W. J., and Mizunaga, T. (1991) Glycosylation site binding protein and protein disulfide isomerase are identical and essential for cell viability in yeast, *Proc. Natl. Acad. Sci. U.S.A. 88*, 4453−4457.
23. Scherens, B., Dubois, E., and Messenguy, F. (1991) Determination of the sequence of the yeast *YCL313* gene localized on chromosome III. Homology with the protein disulfide isomerase (PDI gene product) of other organisms, *Yeast 7*, 185−193.
24. Tachikawa, H., Miura, T., Katakura, Y., and Mizunaga, T. (1991) Molecular structure of a yeast gene, *PDI1*, encoding protein disulfide isomerase that is essential for cell growth, *J. Biochem. 110*, 306−313.
25. Woycechowsky, K. J., and Raines, R. T. (2000) Native disulfide bond formation in proteins, *Curr. Opin. Chem. Biol. 4*, 533−539.
26. Sevier, C. S., and Kaiser, C. A. (2002) Formation and transfer of disulphide bonds in living cells, *Nat. Rev. Mol. Cell Biol. 3*, 836−847.
27. Tu, B. P., and Weissman, J. S. (2004) Oxidative protein folding in eukaryotes: Mechanisms and consequences, *J. Cell Biol. 164*, 341−346.
28. Laboissière, M. C. A., Sturley, S. L., and Raines, R. T. (1995) The essential function of protein-disulfide isomerase is to unscramble non-native disulfide bonds, *J. Biol. Chem. 270*, 28006−28009.
29. Walker, K. W., Lyles, M. M., and Gilbert, H. F. (1996) Catalysis of oxidative protein folding by mutants of protein disulfide isomerase with a single active-site cysteine, *Biochemistry 35*, 1972−1980.
30. Tachibana, C., and Stevens, T. H. (1992) The yeast *EUG1* gene encodes an endoplasmic reticulum protein that is functionally related to protein disulfide isomerase, *Mol. Cell. Biol. 12*, 4601−4611.
31. Chivers, P. T., Laboissière, M. C. A., and Raines, R. T. (1996) The CXXC motif: Imperatives for the formation of native disulfide bonds in the cell, *EMBO J. 16*, 2659−2667.
32. Xiao, R., Solovyov, A., Gilbert, H. F., Holmgren, A., and Lundström-Ljung, J. (2001) Combinations of protein-disulfide isomerase domains show that there is little correlation between isomerase activity and wild-type growth. *J. Biol. Chem. 276*, 27975−27980.
33. Solovyov, A., Xiao, R., and Gilbert, H. F. (2004) Sulfhydryl oxidation, not disulfide isomerization, is the principal function of protein disulfide isomerase in yeast *Saccharomyces cerevisiae*, *J. Biol. Chem. 279*, 34095−34100.
34. Xiao, R., Wilkinson, B., Solovyov, A., Winther, J. R., Holmgren, A., Lundström-Ljung, J., and Gilbert, H. F. (2004) The contributions of protein disulfide isomerse and its homologs to oxidative protein folding in the yeast ER, *J. Biol. Chem. 279*, 49780−49786.
35. Narayan, M., Welker, E., Wedemeyer, W. J., and Scheraga, H. A. (2000) Oxidative folding of proteins, *Acc. Chem. Res. 33*, 805−812.
36. Walker, K. W., and Gilbert, H. F. (1997) Scanning and escape during protein-disulfide isomerase-assisted protein folding, *J. Biol. Chem. 272*, 8845−8848.
37. Schwaller, M., Wilkinson, B., and Gilbert, H. F. (2003) Reduction/reoxidation cycles contribute to catalysis of disulfide isomerization by protein disulfide isomerase, *J. Biol. Chem. 278*, 7154−7159.
38. Goldberger, R. F., Epstein, C. J., and Anfinsen, C. B. (1963) Acceleration of reactivation of reduced bovine pancreatic ribonuclease by a microsomal system from rat liver, *J. Biol. Chem. 238*, 628−635.
39. Raines, R. T. (1998) Ribonuclease A, *Chem. Rev. 98*, 1045−1065.
40. Chivers, P. T., Laboissière, M. C. A., and Raines, R. T. (1998) Protein disulfide isomerase: Cellular enzymology of the CXXC motif, in *Prolyl Hydroxylase, Protein Disulfide Isomerase, and Other Structurally Related Proteins* (Guzman, N. A., Ed.) pp 487−505, Marcel Dekker, New York.
41. Gilbert, H. F. (1998) Protein disulfide isomerase, *Methods Enzymol. 290*, 26−50.
42. Konishi, Y., Ooi, T., and Scheraga, H. A. (1981) Regeneration of ribonuclease A from the reduced protein. Isolation and identification of intermediates and equilibrium treatment, *Biochemistry 20*, 3945−3955.
43. Freedman, R. B., Klappa, P., and Ruddock, L. W. (2003) Model peptide substrates and ligands in analysis of action of mammalian protein disulfide-isomerase, *Methods Enzymol. 348*, 342−354.
44. Darby, N. J., Freedman, R. B., and Creighton, T. E. (1994) Dissecting the mechanism of protein disulfide isomerase: Catalysis of disulfide bond formation in a model peptide, *Biochemistry 33*, 7937−7947.
45. Ruddock, L. W., Hirst, T. R., and Freedman, R. B. (1996) pH-Dependence of the dithiol-oxidizing activity of DsbA (a periplasmic protein thiol:disulphide oxidoreductase) and protein disulphide-isomerase: Studies with a novel simple peptide substrate, *Biochem. J. 315*, 1001−1005.
46. Alanen, H. I., Williamson, R. A., Howard, M. J., Lappi, A.-K., Jäntti, H. P., Rautio, S. M., Kellokumpu, S., and Ruddock, L. W. (2003) Functional characterization of ERp18, a new endoplasmic reticulum-located thioredoxin superfamily member, *J. Biol. Chem. 278*, 28912−28920.
47. Christiansen, C., St. Hilaire, P. M., and Winther, J. R. (2004) Fluorometric poly(ethylene glycol)-peptide hybrid substrates for quantitative assay of protein disulfide isomerase, *Anal. Biochem. 333*, 148−155.
48. Cline, D. J., Thorpe, C., and Schneider, J. P. (2004) Structure-based design of a fluorimetric redox active peptide probe, *Anal. Biochem. 35*, 144−150.
49. Lappi, A. K., Lensink, M. F., Alanen, H. I., Salo, K. E. H., Lobell, M., Juffer, A. H., and Ruddock, L. W. (2004) A conserved arginine plays a role in the catalytic cycle of the protein disulphide isomerases, *J. Mol. Biol. 335*, 283−295.
50. Pedone, E., Ren, B., Ladenstein, R., Rossi, M., and Barolucci, S. (2004) Functional properties of the protein disulfide oxidoreductase from the archaeon *Pyrococcus furiosis*. A member of a novel protein family related to protein disulfide-isomerase, *Eur. J. Biochem. 271*, 3427−3448.

51. Lee, K., Dzubeck, V., Latshaw, L., and Schneider, J. P. (2004) De novo designed peptidic redox potential probe: Linking sensitized emission to disulfide bond formation, *J. Am. Chem. Soc. 126*, 13616−13617.
52. Nakamura, T., Furunaka, H., Miyata, T., Tokunaga, F., Muta, T., Iwanaga, S., Niwa, M., Takao, T., and Shimonishi, Y. (1988) Tachyplesin, a class of antimicrobial peptide from the hemocytes of the horseshoe crab (*Tachypleus tridentatus*). Isolation and chemical structure, *J. Biol. Chem. 263*, 16709−16713.
53. Kawano, K., Yoneya, T., Miyata, T., Yoshikawa, K., Tokunaga, F., Terada, Y., and Iwanaga, S. (1990) Antimicrobial peptide, tachyplesin I, isolated from hemocytes of the horseshoe crab (*Tachypleus tridentatus*). NMR determination of the β-sheet structure, *J. Biol. Chem. 265*, 15365−15367.
54. Laederach, A., Andreotti, A. H., and Fulton, D. B. (2002) Solution and micelle-bound structures of tachyplesin I and its active aromatic linear derivatives, *Biochemistry 41*, 12359−12368.
55. Matsuzaki, K., Yoneyama, S., Fujii, N., Miyajima, K., Yamada, K., Kirino, Y., and Anzai, K. (1997) Membrane permeabilization mechanisms of a cyclic antimicrobial peptide, tachyplesin I, and its linear analog, *Biochemistry 36*, 9799−9806.
56. Oishi, O., Yamashita, S., Nishimoto, E., Lee, S., Sugihara, G., and Ohno, M. (1997) Conformations and orientations of aromatic amino acid residues of tachyplesin I in phospholipid membranes, *Biochemistry 36*, 4352−4359.
57. Annis, I., Hargittai, B., and Barany, G. (1997) Disulfide bond formation in peptides, *Methods Enzymol. 289*, 198−221.
58. Tamamura, H., Otaka, A., Nakamura, J., Okubo, K., Koide, T., Ikeda, K., and Fujii, N. (1993) Disulfide bond formation in *S*-acetamidomethyl cysteine-containing peptides by the combination of silver trifluoromethanesulfonate and dimethyl sulfoxide/aqueous HCl, *Tetrahedron Lett. 34*, 4931−4934.
59. Tamamura, H., Otaka, A., Nakamura, J., Okubo, K., Koide, T., Ikeda, K., Ibuka, T., and Fujii, N. (1995) Disulfide bond-forming reaction using a dimethyl sulfoxide/aqueous HCl system and its application to regioselective two disulfide bond formation, *Int. J. Pept. Protein Res. 45*, 312−319.
60. Tamamura, H., Matsumoto, F., Sakano, K., Otaka, A., Ibuka, T., and Fujii, N. (1998) Unambiguous synthesis of stromal cell-derived factor-1 by regioselective disulfide bond formation using a DMSO-aqueous HCl system, *Chem. Commun. 1998*, 151−152.
61. Gill, S. C., and von Hippel, P. H. (1989) Calculation of protein extinction coefficients from amino acid sequence data, *Anal. Biochem. 182*, 319−326.
62. Rabbani, L. D., Pagnozzi, M., Chang, P., and Breslow, E. (1982) Partial digestion of neurophysins with proteolytic enzymes: Unusual interactions between bovine neurophysin II and chymotrypsin, *Biochemistry 21*, 817−826.
63. Lees, W. J., and Whitesides, G. M. (1993) Equilibrium constants for thiol−disulfide interchange reactions: A coherent, corrected set, *J. Org. Chem. 58*, 642−647.
64. Kunkel, T. A. (1985) Rapid and efficient site-specific mutagenesis without phenotypic selection, *Proc. Natl. Acad. Sci. U.S.A. 82*, 488−492.
65. Laboissière, M. C. A., Chivers, P. T., and Raines, R. T. (1995) Production of rat protein disulfide isomerase in *Saccharomyces cerevisiae*, *Protein Expression Purif. 6*, 700−706.
66. Woycechowsky, K. J., Wittrup, K. D., and Raines, R. T. (1999) A small-molecule catalyst of protein folding *in vitro* and *in vivo*, *Chem. Biol. 6*, 871−879.
67. Lundström, J., and Holmgren, A. (1993) Determination of the reduction−oxidation potential of the thioredoxin-like domains of protein disulfide-isomerase from the equilibrium with glutathione and thioredoxin, *Biochemistry 32*, 6649−6655.
68. Lakowicz, J. R., Gryczynski, I., Wiczk, W., Laczko, G., Prendergast, F. C., and Johnson, M. L. (1990) Conformational distributions of melittin in water/methanol mixtures from frequency-domain measurements of nonradiative energy transfer, *Biophys. Chem. 36*, 99−115.
69. Eis, P. S., and Lakowicz, J. R. (1993) Time-resolved energy transfer measurements of donor−acceptor distance distributions and intramolecular flexibility of a CCHH zinc finger peptide, *Biochemistry 32*, 7981−7993.
70. Maliwal, B. P., Lakowicz, J. R., Kupryszewski, G., and Rekowski, P. (1993) Fluorescence study of conformational flexibility of RNase S-peptide: Distance-distribution, end-to-end diffusion, and anisotropy decays, *Biochemistry 32*, 12337−12345.
71. Lakowicz, J. R., Gryczynski, I., Laczko, G., Wiczk, W., and Johnson, M. L. (2004) Distribution of distances between the tryptophan and the N-terminal residue of melittin in its complex with calmodulin, troponin C, and phospholipids, *Protein Sci. 3*, 628−637.
72. Akaji, K., Tatsumi, T., Yoshida, M., Kimura, T., Fujiwara, Y., and Kiso, Y. (1992) Disulfide bond formation using the silyl chloride-sulfoxide system for the synthesis of a cystine peptide, *J. Am. Chem. Soc. 114*, 4137−4143.
73. Akaji, K. (1997) Disulfide bond formation using silyl chloride-sulfoxide system, *Rev. Heteroat. Chem. 16*, 85−100.
74. Cuthbertson, A., and Indrevoll, B. (2000) A method for the one-pot regioselective formation of the two disulfide bonds of α-conotoxin SI, *Tetrahedron Lett. 41*, 3661−3663.
75. Kamber, B., Hartmann, A., Eisler, K., Riniker, B., Rink, H., Sieber, P., and Rittel, W. (1980) The synthesis of cystine peptides by iodine oxidation of *S*-trityl-cysteine and *S*-acetamidomethyl-cysteine peptides, *Helv. Chim. Acta 63*, 899−915.
76. Sieber, P., Kamber, B., Riniker, B., and Rittel, W. (1980) Iodine oxidation of *S*-trityl-cysteine-peptides and *S*-acetamidomethyl-cysteine-peptides containing tryptophan—Conditions leading to the formation of tryptophan-2-thioethers, *Helv. Chim. Acta 63*, 2358−2363.
77. Hawkins, H. C., and Freedman, R. B. (1991) The reactivities and ionization properties of the active-site dithiol groups of mammalian protein disulphide-isomerase, *Biochem. J. 275*, 335−339.
78. Cleland, W. W. (1964) Dithiothreitol, a new protective reagent for SH groups, *Biochemistry 3*, 480−482.
79. Krause, G., Lundström, J., Barea, J. L., Pueyo de la Cuesta, C., and Holmgren, A. (1991) Mimicking the active site of protein disulfide-isomerase by substitution of proline 34 in *Escherichia coli* thioredoxin, *J. Biol. Chem. 266*, 9494−9500.
80. Weissman, J. S., and Kim, P. S. (1993) Efficient catalysis of disulphide bond rearrangements by protein disulphide isomerase, *Nature 365*, 185−188.
81. Lyles, M. M., and Gilbert, H. F. (1991) Catalysis of the oxidative folding of ribonuclease A by protein disulfide isomerase: Dependence of the rate on the composition of the redox buffer, *Biochemistry 30*, 613−619.
82. Rabenstein, D. L. (1973) Nuclear magnetic resonance studies of the acid−base chemistry of amino acids and peptides. I. Microscopic ionization constants of glutathione and methylmercury-complexed glutathione, *J. Am. Chem. Soc. 95*, 2797−2803.
83. Lyles, M. M., and Gilbert, H. F. (1994) Mutations in the thioredoxin sites of protein disulfide isomerase reveal functional nonequivalence of the N- and C-terminal domains, *J. Biol. Chem. 269*, 30946−30952.
84. Darby, N. J., and Creighton, T. E. (1995) Characterization of the active site cysteine residues of the thioredoxin-like domains of protein disulfide isomerase, *Biochemistry 34*, 16770−16780.

BI0507985